Chemosphere 352 (2024) 141409

Contents lists available at ScienceDirect

Chemosphere

journal homepage: www.elsevier.com/locate/chemosphere

Lavandula multifida as a novel eco-friendly fluorescent-blue material for mercury ions sensing in seawater at femto-molar concentration

MeryamChelly [a,b], Sabrine Chelly [a,b], Angelo Ferlazzo [a,c], Giovanni Neri [a,*], Hanen Bouaziz-Ketata [b,**]

[a] Department of Engineering, University of Messina, C.da Di Dio, I-98166, Messina, Italy
[b] Laboratory of Toxicology-Microbiology Environmental and Health, LR17ES06, Sfax, Tunisia
[c] Department of Chemical Sciences, University of Catania, Viale A. Doria 6, 95125, Catania, Italy

HIGHLIGHTS

- A novel fluorescent material based on the herbal tea of *Lavandula multifida* (*Lm*) is presented.
- A *Lm*-Nafion on polyethylene terephthalate (PET) fluorescent probe sensor has been developed.
- Highly sensitive and selective sensing of Hg^{2+} was achieved.
- Exceptional low detection limit (LOD) of 0.25 fM for Hg^{2+} ions in seawater was reported.

GRAPHICAL ABSTRACT

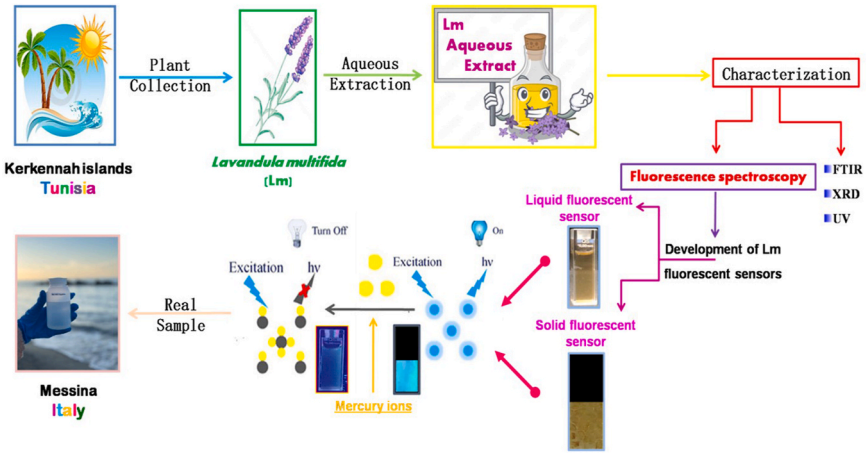

ARTICLE INFO

Handling Editor: Grzegorz Lisak

Keywords:
Lavandula multifida
Fluorescent sensor
Mercury ions
Seawater

ABSTRACT

In this paper, we present a novel fluorescent material based on the herbal tea of *Lavandula multifida* (*Lm*). The fluorescence properties of *Lm* aqueous extract were analyzed under various excitation wavelengths in the range of 290–450 nm. The *Lm* herbal infusion was found to be highly fluorescent, with an emission maximum at 450 nm under excitation at 390 nm. Consequently, it was exploited to develop a fluorescence method for detecting metal ions. Results obtained upon the addition of Hg^{2+}, Na^{+}, K^{+}, Ca^{2+}, Mg^{2+}, Pb^{2+}, Cd^{2+}, Cu^{2+}, Ni^{2+}, Bi^{3+}, Mn^{2+}, Fe^{3+} and Co^{2+} ions showed that the fluorescence intensity of the *Lm* aqueous extract decreased strongly with the presence of mercury ions. A solid-state fluorescent sensor, based on *Lm* embedded into a Nafion membrane and deposited on a transparent polyethylene terephthalate (PET) sheet, has also been developed for the effective detection of Hg^{2+} ions. The *Lm*-Nafion-PET sensor exhibited good stability, high repeatability, and reproducibility. Furthermore, the *Lm*-Nafion/PET sensor demonstrated remarkable sensitivity to Hg^{2+} in sea

* Corresponding author.
** Corresponding author.
E-mail addresses: gneri@unime.it (G. Neri), hanenktata@yahoo.fr (H. Bouaziz-Ketata).

https://doi.org/10.1016/j.chemosphere.2024.141409
Received 10 December 2023; Received in revised form 30 January 2024; Accepted 6 February 2024
Available online 10 February 2024

water, with a limit of detection of 0.25 fM. To our knowledge, this is the first study which reports *Lavandula multifida* plant for making a novel eco-friendly fluorescent solid-state sensor for the detection of mercury ions at femto-molar concentrations in seawater.

Abbreviations

Lm	Lavandula multifida
PET	PolyethyleneTerephthalate
BF	Blue fluorescence
GF	Green fluorescence
Hg^{2+}	Mercury ion
Na^{+}	Sodium ion
K^{+}	Potassium ion
Ca^{2+}	Calcium ion
Mg^{2+}	Magnesium ion
Pb^{2+}	Plomb ion
Cd^{2+}	Cadmium ion
Cu^{2+}	Copper ion
Ni^{2+}	Nickel ion
Bi^{3+}	Bismuth ion
Mn^{2+}	Manganese ion
Fe^{3+}	Iron ion
Co2+	Cobalt ion
LOD	Limit of detection
UV–Vis	Ultraviolet–visible
FTIR	Fourier TransformInfraredSpectroscopy
IR	Infrared
XRD	nM μM fM X-ray powder diffraction Nanomolar Micromolar Femtomolar

1. Introduction

Chemical sensors have become indispensable in modern society, revolutionizing various sectors including healthcare, environmental protection, forensics, pharmaceuticals, clinical diagnostics, automotive, food safety, and agriculture (Javaid et al., 2021). These devices have several advantages, being low-cost, portable, and simple to use. Among the various types of chemical sensors available, fluorescent sensors stand out as label-free tools capable of detecting molecules that emit light in response to specific stimuli (Demchenko, 2008). This unique property makes them exceptionally sensitive and enables a wide range of applications, from studying biological processes to analyzing metal ions in environmental samples and monitoring pH changes (Adair et al., 2022; Donaldson, 2020; Du et al., 2019).

Among these, mercury metal ions detection using kiwi peel aqueous extract fluorophores (Sun et al., 2021) and copper ions using willow seeds luminescent dyes (Yang et al., 2022), are just few examples to mention. Mercury ions contamination in water is an issue to the environment and human health. Since the 1970s, extensive field investigations worldwide, including the Mediterranean region, to assess mercury ions concentrations in sea water and/or marine organisms, and studies on its impact on human well-being, have been conducted. Some studies have revealed significantly higher mercury levels in specific fish species in the Mediterranean compared to the Atlantic Ocean. These scientific efforts have led to the development of advanced analytical and modeling techniques, enabling comprehensive regional assessments of mercury's spatial and temporal dynamics in living organisms and the environment. Despite these efforts, there are still gaps in our understanding of the processes influencing mercury behavior and its sources, particularly in the environment (Cinnirella et al., 2019).

Here, we report an unprecedented study on *Lavandula multifida* (*Lm*) plant as a natural fluorescent dye for developing a fluorescent sensor. This plant grows spontaneously in Kerkennah, a small archipelago of ten islands located in the southwestern part of the Strait of Sicily (Italy) and the Southeast of Tunisia (Neji et al., 2018). The archipelago represents an exceptional biodiversity reservoir and serves as a refuge for a quarter of Mediterranean species (fauna and flora) (Chatenoux et al., 2015). Lavender has been extensively used by the inhabitants of the islands in folk medicine and as a food flavoring. The genus Lavandula, belonging to the Lamiaceae family, has remarkably attracted scientists' interest. As a plant food, particular attention has been given to the tea infusions (i.e., aqueous extracts) of lavender, which have been shown to have multidirectional biological activities such as antidepressant, antitumor, anti-inflammatory, antioxidant, and antiviral properties, which are thought to be explained by their richness in a wide range of bioactive aqueous phenolic molecules, e.g., phenolic acids, flavonoids, anthocyanins, and tannins (Lopes et al., 2018; Kageyama et al., 2012).

Despite the extensive research on Lavender species, their potential as fluorescent materials remain largely unexplored. Therefore, our work presents, for the first time, the isolation of *Lavandula multifida* from the Kerkennah Islands and its application as a natural, eco-friendly fluorescent material. We demonstrate the use of *Lm* extract in developing a solid-state fluorescent sensor for monitoring heavy mercury ions, employing Nafion as an entrapping membrane on a flexible PET sheet substrate.

2. Materials and methods

2.1. Reagents

All chemicals used were of analytical reagent grade. Doubly distilled water was used throughout. Heavymetal solutions at different concentrations were prepared from their standard stock solutions.

2.2. Plant collection

*Lavandula multifida*aerial part was collected in March 2022 from Kerkennah islands (Sfax, Tunisia), located in the southwestern part of the Strait of Sicily (Italy) and the Southeast of Tunisia (Latitude: 34° 43′ 59.99" North; Longitude: 11° 13' 60.00" East, Tunisia) (Fig. 1).

A voucher specimen (voucher n° B18/2022) authenticated by Prof. Mohamed Chaieb (Laboratory of Vegetal Biology, Faculty of Sciences of Sfax, Tunisia), was deposited at the Faculty of Sciences (Sfax, Tunisia).

2.3. Plant extraction

The aerial parts of Lavandula multifida were carefully dried for 2 weeks and then ground into a fine powder. A quantity of 500 mg of the coarse powder was extracted using 100 mL of distilled water and macerated for 30 min at room temperature with occasional shaking. The resulting macerate was then filtered using Whatman filter paper N°1 and stored at 25 °C in a dark glass container for further analysis (Chelly et al., 2021).

2.4. Characterization

Infrared (IR) spectra were recorded in the range of 4500 to 500 cm^{-1}, with a resolution of 4 cm^{-1} using a PerkinElmer Spectrum 100 spectrometer. X-ray diffraction (XRD) spectra were obtained using an X-ray diffractometer (Bruker D8 Advance A 25) at a potential of 40 kV and a 2-theta range of 20–80, with an increment rate of 0.01°/s. UV–Vis spectroscopy was performed in the wavelength range of 250–900 nm using a PerkinElmer Lambda 25 UV-VIS spectrophotometer (Satira et al., 2021).

2.5. Solid state sensor fabrication

To fabricate the solid-state fluorescent sensor, we utilized a transparent and flexible polyethylene terephthalate (PET) sheet measuring approximately 10 × 30 × 0.3 mm. This sheet was then coated by drop-casting with an appropriate volume of *Lm* dye aqueous solution. Additionally, Nafion was introduced to entrap the dye and enhance its adhesion to the PET sheet surface. Subsequently, a blank ink was printed to demarcate the dye-sensing zone. The modified *Lm*-Nafion/PET sensor was left to dry at room temperature before being utilized for further experiments.

2.6. Photoluminescence measurements

A spectrophotometer (NanoLog modular (Horiba)) was used to excite the *Lm* aqueous extract at different excitation wavelengths. The fluorescence emission spectra were recorded in triplicate. The effect of metal ions on the fluorescence emission spectrum of *Lm* aqueous extract was evaluated by adding Hg^{2+}, Na^{+}, K^{+}, Ca^{2+}, Mg^{2+}, Pb^{2+}, Cd^{2+},Cu^{2+}, Ni^{2+}, Bi^{3+}, Mn^{2+}, $Fe^{3+}$and Co^{2+} in the concentration range of 0–10000 nM under excitations at 390 nm. All experiments were performed in triplicate at room temperature (Iannazzo et al., 2021). Additionally, a portable UV lamp was used to irradiate the solid-state sensor at a wavelength of 365 nm.

3. Results and discussion

3.1. Lavandula multifida plant characterization

The *Lm* sample was first characterized by FT-IR and XRD analysis. FT-IR is a technique that provides important indications about the functional groups present in plants. Fig. 2a shows the IR fingerprint of *Lm* powder. Among all the bands observed in the IR spectra, the absorption at 3306 cm^{-1} is due to the stretching of hydroxyl groups (O–H stretching) of phenol constituents in the *Lm* plant. The band at 2932 cm^{-1} is attributed to the C–H symmetric stretching (alkane). A band at 2317 cm^{-1} is assigned to O═C═O stretching vibration (carbon dioxide), and that at 2083 cm^{-1} is due to the stretching vibration of N═C═S (isothiocyanate). The peak at 1622 cm^{-1} corresponds to C═C stretching (conjugated alkene). The band at 1395 cm^{-1} indicates the presence of carboxylic acid with O–H stretching vibrations. The band at 1245 cm^{-1} is assigned to C–O stretching (aromatic ester). A notable band at 1024 cm^{-1} can be assigned to C–O stretching. The peak noticed at 533 cm^{-1} is due to C–I stretching (halo compound) (https://www.sigmaaldrich.com/TN/en/technical-documents/technical-article/analytical-chemistry/photometry-and-reflectometry/ir-spectrum-table.). The FTIR spectrum revealed the presence of polyphenols and flavonoids due to O–H stretching and terpenes due to CH groups (Dhivya et al., 2017). All these compounds, belonging to secondary plant metabolites, could be responsible for the fluorescent properties of *Lavandula multifida* (Dobros et al., 2022).

The crystalline structure of the *Lm* sample was assessed by XRD analysis (Fig. S1). The XRD pattern of the *Lm* plant revealed two peaks at 14.78 and 22.03 and an intense one at 39.4, assigned to the {100} plane. These peaks can be related to the reflection of crystalline cellulose in *Lm* lignocellulosic biomass (Satira et al., 2021).

In this regard, *Lavandula multifida* can be considered a source of crystalline cellulose known to be employed in several fields, such as nanocomposite materials, biomedical products, electroactive polymers, supercapacitors, templates for electronic components, batteries, catalytic supports, etc. (Kim et al., 2013).

3.2. Optical characterization of Lavandula multifida aqueous extract

The fluorescent characteristics of the *Lm* aqueous extract were then analyzed. First, the emission-excitation fluorescence data are shown in the 3D graph provided in Fig. 2b. 3D fluorescence spectroscopy generates multidimensional data that help to better understand luminescent properties, especially when analyzing complex real samples, such as plants (Locquet et al., 2006). According to the emission–excitation matrix (EEM) reported in Fig. 2c, many components are clearly visible. Rayleigh scattering (elastic scattering, which shows up as a line in the contour map) with λem = λexc, and its high intensity is related to the solvent and phyto-components in the *Lm* extract. We note a large region of fluorescence emission between 400 and 600 nm, attributed to the presence of many fluorescent molecules in the aqueous extract of *Lm*, and the second-order scattering peak, which appears at various excitation wavelengths as a line with λem = 2 λexc. The emission spectra under different excitation wavelengths are shown in Fig. 2d. PL data collected in the 400–600 nm range show a maximum excitation peak around 448 nm at the excitation wavelengths of 390 nm. This peak is slightly blue-shifted with the decrease of excitation wavelength.

Based on the results obtained, we opted for an excitation wavelength

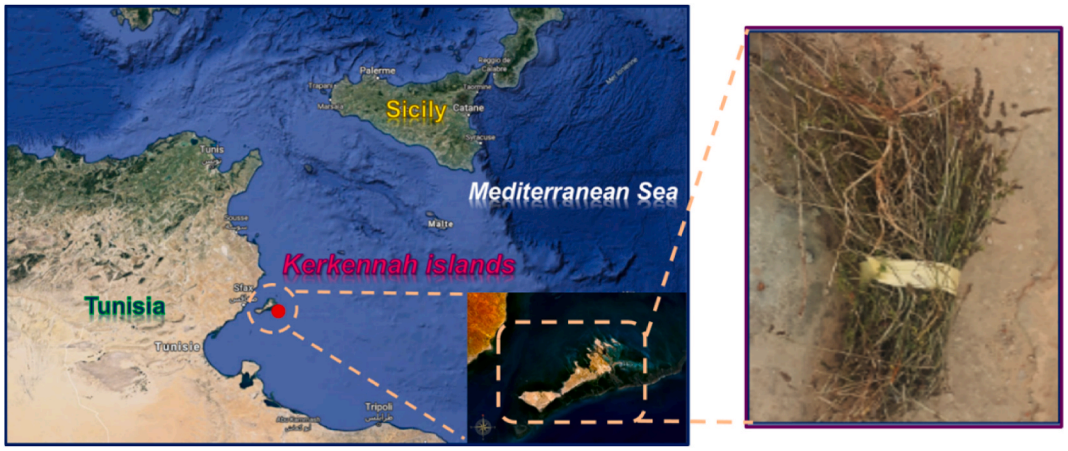

Fig. 1. *Lavandula multifida* plant collection region.

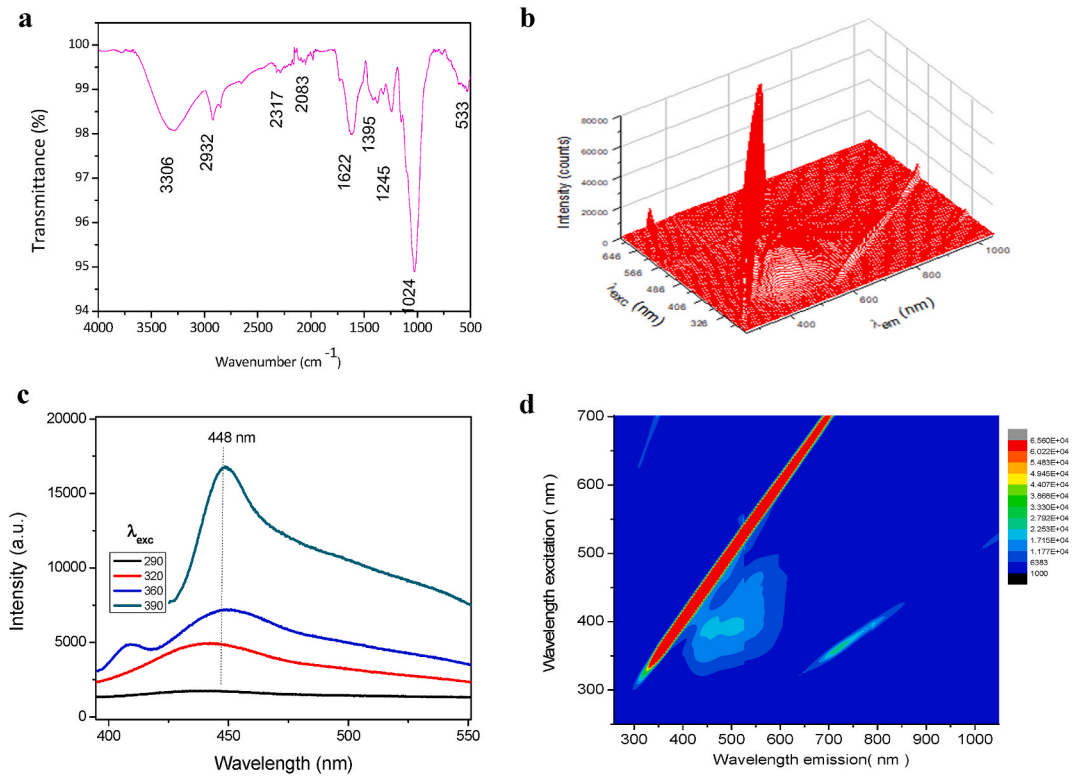

Fig. 2. a) FTIR spectrum of *Lavandula multifida*; **b)** 3D fluorescence spectroscopy; **c)** emission–excitation matrix (EEM); **d)** Fluorescence emission spectra under different excitation wavelengths analysis of *Lavandula multifida* aqueous extract.

(λexc) of 390 nm for subsequent tests. The fluorescence emission spectrum and UV–Vis spectrum of the *Lavandula multifida* aqueous extract are depicted in Fig. 3a. A blue fluorescence (BF) peak at approximately 448 nm is accompanied by a green fluorescence (GF) peak, which appears as a secondary maximum/shoulder at around 530 nm. These observations are consistent with the fluorescence emission spectra documented in the literature (Lang et al., 1991).

As shown, the ultraviolet–visible (UV–Vis) spectrum of the *Lm* extract shows an absorbance peak at 240 nm. This peak is attributed to the π–π* electronic transition of the aromatic carbon bonds (Huang et al., 2019). Visually, the prepared *Lm* aqueous extract has the appearance of a transparent, uniform, and yellow solution under normal light. However, under UV lamp light at 365 nm, the *Lm* extract shows blue emission, corresponding to the blue fluorescence as shown in Fig. 3b.

Our findings are in good accordance with several literature studies (Lang et al., 1991). The origin of the blue fluorescence (BF) could be attributed to specific endogenous plant substances (secondary products) termed phenolic components. In fact, herbal teas from the genus Lavender were described as very rich in total phenolic content (Lopes et al., 2018; Kageyama et al., 2012; Nogués et al., 2000; Radu et al., 2019). Qualitatively, as BF emission (λ_{max} 450 nm) candidates, we can report lignin, phenolic acids (e.g. ferulic acid, caffeic acid, p-coumaric acid, and rosmarinic acid), flavonoids (apigenin, catechin, and luteolin), anthocyanins, tannins, and sporopollenins (Du et al., 2019; Lang et al., 1991). Surprisingly, all the above-cited organic fluorophores were detected in the Lavandula genus. Taking them one by one, many researchers shed light on the huge amount of lignin in Lavender, which is

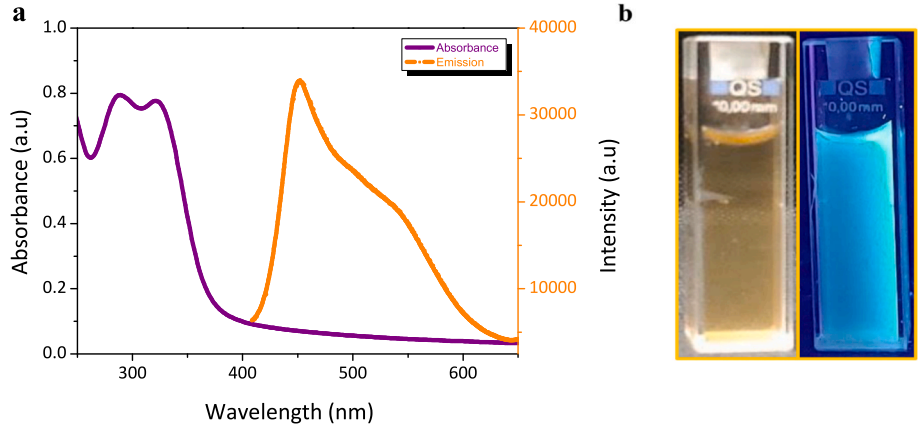

Fig. 3. a) UV–Vis absorption and fluorescence emission spectra at 390 nm excitation of *Lavandula multifida* aqueous extract, **b)** *Lavandula multifida* herbal tea under visible and UV (365 nm) lamp light.

the most abundant ingredient (Vasileva et al., 2018). Known as a large complex polyphenolic biomolecule, lignin is one of the two most important luminescent plant substances. Indeed, it is reported (Du et al., 2019) that the structural components contributing to its fluorescence are conjugated bonds and phenolic rings. Lignin is characterized by a broad emission range due to the functional diversity in numerous organic fluorophore constituents (Du et al., 2019). This may further explain the strong dependence on the excitation wavelength shown by the *Lm* extract. Moreover, the natural polymer fluorescence is influenced by its physical structure (restrictions on intramolecular rotation and clustering of carbonyl groups) and molecular environment, such as quenching agents, attracting our attention to the recommended use of plants rich in lignin as a potential natural fluorescent biosensor.

In addition to lignin, studies have detected significant concentrations of phenolic acids such as ferulic acid, caffeic acid, p-coumaric acid, and especially rosmarinic acid, as well as flavonoids, particularly glycosides like apigenin, catechin, and luteolin, in hydrolyzed extracts of Lavender (Lopes et al., 2018; Kageyama et al., 2012). Other soluble pigments, such as anthocyanins, tannins, and sporopollenins (Du et al., 2019), are also described in large amounts in the Lavender genus. These latter compounds are biopolymers found in flowers (spores and pollen) and are known as characteristic parts of Lavender plants (Radu et al., 2019).

Besides optimizing the highest *Lm* fluorescence intensity, the fluorescence stability represents one of the key properties for optimal working conditions. To evaluate the stability of *Lm* extract fluorescence, we performed daily tests for one week. As shown in Figs. S2a and a remarkable increase in fluorescence was observed within the first 24 h, followed by stabilization in the next 3 days, and a drastic decrease from the fifth day onwards, remaining relatively stable thereafter.

To understand the fluorescent behavior of the *Lm* aqueous extract, pH measurements were also performed (Fig. S2b). It was noted that in the first 4 days following the extraction, both photoluminescence and pH (initially slightly acidic) increased to reach maximum fluorescence intensity and almost neutral pH values (6.40–7.00). This may be explained by the fact that polyphenols present in the *Lm* aqueous extract are unstable and rapidly transform into various reaction products during post-harvesting and processing (Cao et al., 2021). Considering no external factors (such as temperature, pH, light, etc.), this instability could be dramatically affected by their structural variations (Cao et al., 2021). Secondly, being in water, the oxygen transfer rate increases, hence leading to autoxidation which accelerates the degradation reactions of the phenolic compounds and subsequently increases pH (Cao et al., 2021). Furthermore, non-lyophilized molecules undergo continuous chemical reactions such as pigmentation, glycosylation, hydroxylation, alkylation, carboxymethylation, methylation/condensation, amination, and so on, giving rise to the formation of fluorescent byproducts (Cao et al., 2021). In addition, breaking down covalent linkages between lignin and hemicellulose; abundant polymers in the Lavender genus, could induce an increase in *Lm* fluorescence brightness (Vasileva et al., 2018; Członka et al., 2021). Like our findings, Jiang et al. (2021) demonstrated that the novel synthesized dicoumarin-Hg fluorescent probe showed a stable fluorescence intensity in the pH range of 6.40–7.00. Starting from the fifth day, fluorescence intensity decreases remarkably. According to the literature, alkaline pH can intensively weaken the stability of some molecules such as anthocyanins, flavonoids, and phenolic acids, resulting in quasi-total fluorescence quenching (He et al., 2015). So, the observed change in fluorescence can be related to the increase in pH attributed to the degradation of some molecules in the aqueous extract. In conclusion, polymeric intermediates formed may change the pH of the solution (Zhu, 2015), which in turn exhibits negative feedback that may alter the molecules' structure, and consequently their stability and fluorescent properties. To the best of our knowledge, the present work discusses, for the first time, the relationship between fluorescence intensity and pH in *Lavandula multifida* infusion tea.

As a result, the *Lm* aqueous extract exhibited the highest fluorescent intensity during the first 4 days of storage at pH 6.04–7.00 in the dark at room temperature. In addition to the fixed suitable storage conditions, it is also necessary to mention the importance of the chosen extraction process, i.e., maceration, which is known as the most affordable and promising approach to successfully obtain fluorescent molecules. This conventional technique is one of the go-to methods due to its environmentally friendly characteristics, using water as a solvent, simplicity, low cost, low temperatures, shorter duration, and minimal experimental setup required (Sridhar et al., 2021).

3.3. Metal ions detection with Lm aqueous extract

It is well known that plant extracts containing polyphenols show high selectivity for Hg^{2+} over other metal ions, providing a rationale for utilizing them in the development of mercury sensors (Sridhar et al., 2021). To evaluate the characteristics of *Lm* extract as a fluorescent material for detecting metal ions, stock solutions of different relevant metal ions, including Hg^{2+}, Na^{+}, K^{+}, Ca^{2+}, Mg^{2+}, Pb^{2+} Cd^{2+},Cu^{2+}, Ni^{2+}, Bi^{3+}, Mn^{2+}, Fe^{3+} and Co^{2+}, were added to *Lm* extract, and the fluorescence emission intensities were measured. As clearly observed in Fig. 4a, Hg^{2+} led to a strong suppression of *Lm* fluorescence compared to the other metal ions tested (Fig. 4b).

This result clearly underlines the high performance of *Lavandula multifida* as a novel turn-off type fluorescent probe for Hg^{2+} ions (Shuai et al., 2021; Wang et al., 2021; Şenol et al., 2023). Therefore, *Lavandula multifida* aqueous extract was tested for its quantitative detection. As shown in Fig. 4c, the intensity of fluorescence at 390 nm decreased as the concentration of mercury ions increased in the range of 1–10,000 nM (10 μM). Within this range, two calibration curves could be derived (Fig. 4d). Specifically, the linear regression equations were defined as: $y = 253.35 + 236.23x$ for the lower concentration range and $y = 2410 + 1.223x$ for the higher one. The limit of detection (LOD) was then calculated as $LOD = 3\sigma/k$, where σ is the standard deviation of the mercury ion measurements and k is the slope of the line obtained by plotting fluorescence intensity versus the mercury ion concentration. The calculated LOD value of 2.8 nM demonstrates that the fluorescent *Lm* turn-off behavior is highly sensitive to the presence of Hg^{2+}.

The observed behavior of *Lm* aqueous extract in the presence of mercury ions is likely due to the presence of phenolic blue-fluorescent phytochemicals in this plant (Du et al., 2019). Wei and collaborators mentioned that plant phenolic compounds can strongly chelate various metal ions through the catechol or galloyl groups (Wei et al., 2018). Sun et al. (2021) demonstrated that kiwi peel aqueous extract can detect Hg^{2+} with a limit of detection (LOD) of 1.6 μM. Moreover, silver ions derived from French Lavender, named *Lavandula stoechas*, showed high sensitivity to mercury ions with an LOD value of 2.7 μM (Yılmaz et al., 2021). These examples further demonstrate the superior performance, in terms of LOD, of the fluorescent method using the *Lm* dye.

3.4. Optical properties of Lavandula multifida as solid-state fluorescent sensor

After verifying the performance of *Lavandula multifida* aqueous extract for fluorescence sensing, *Lm* dye was immobilized within a flexible platform with the objective of fabricating a solid-state sensor. This was achieved by coating a PET sheet with the *Lm* probe. Nafion was chosen as a supporting matrix for *Lm* due to its sulfonate groups, which can electrostatically interact with the dye (Marchini et al., 2022), resulting in a transparent, non-fluorescent membrane. Pictures of the Nafion/PET substrate (Fig. 5a) and the *Lm*-Nafion/PET sensor (Fig. 5b) are provided. The *Lm*-Nafion sensor appeared nearly yellow under visible light, which is clearly attributable to the entrapment of *Lm* within the Nafion membrane extract (Singh et al., 2015).

To confirm the fluorescent properties of *Lm* entrapped in the Nafion membrane, we tested the *Lm*-solid sensor under the same conditions as the aqueous extract. As depicted in Fig. 5c, when excited at 390 nm, the

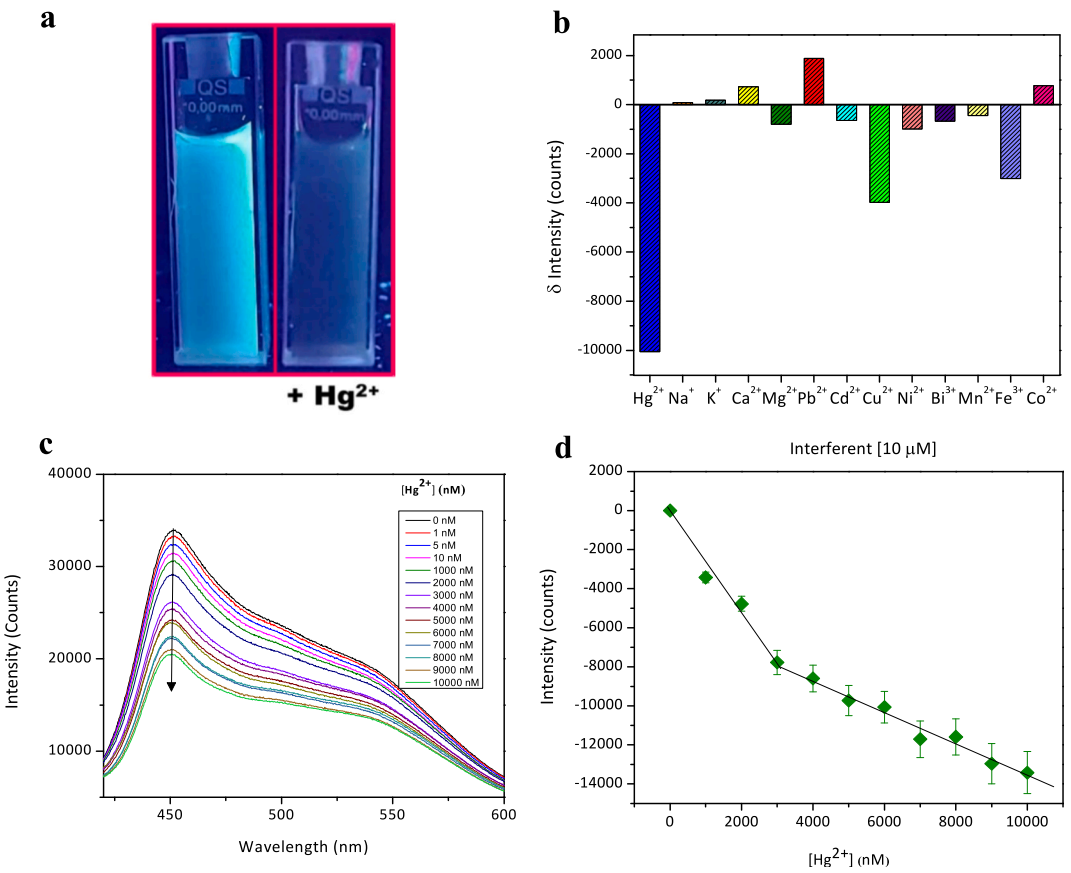

Fig. 4. a) Picture of the irradiated *Lavandula multifida* aqueous extract sample before and after addition of mercury ions; **b**) Comparison of the fluorescence intensity drop of *Lm* sample after addition of different metal ions at the concentration of 10 µM; **c**) response to mercury ions; **d)** calibration curve with error bars derived from measurement carried in triplicate.

fluorescence intensity originating from the Nafion membrane is negligible. However, a prominent emission peak at 450 nm was observed for the *Lm*-Nafion/PET solid-state sensor. The fluorescence spectra obtained in both liquid and solid states are nearly identical, confirming consistent optical behavior (Rebollar et al., 2014).The photoluminescence behavior stability of the developed *Lm*-Nafion sensor has also been checked daily for one week. As shown in Fig. S3a, no remarkable variation in the fluorescence intensity was observed, indicating the good stability of the *Lm* sensor, with an the relative standard deviation (RSD) value equal to 1.679%. It is noteworthy that the fluorescence stability of *Lm* is significantly improved when the dye is embedded in the Nafion structure compared to the *Lm* aqueous extract.

This improved dye stability, when incorporated into the Nafion membrane as compared to an aqueous solution, has also been reported by Mohan et al. (1989). The evaluation of the *Lm* solid sensor's repeatability was determined by a series of three measurements using the same sensor sheet (Fig. S3b). The low value of the RSD (0.997%) indicates good repeatability of the measurements. To evaluate reproducibility, three different sheets coated with the *Lm* probe were tested under the same experimental conditions (Fig. S3c). In this regard, the obtained curves closely overlapped, thus proving high reproducibility of the measurements (RSD equal to 1.035%).

Using a natural product as a sensor probe poses some problems related to reproducibility when aqueous extracts are used from different batches of *Lm*. These challenges hinder their optimal management. This aspect is currently under investigation, along with the study of the contribution of the different parts of the plant (leaf, flower, stem, and root).

3.5. *Lm solid-state fluorescent sensor for mercury detection*

Data obtained suggest that the *Lavandula multifida* solid-state sensor is a promising fluorescent device. Therefore, it was tested for the fluorometric sensing of Hg^{2+}. Preliminarily, it was verified that the fluorescence drop of the *Lm*-Nafion-PET sensor in the presence of mercury ions is remarkably higher compared to the aqueous extract. Thus, tests were carried out with lower concentrations of mercury ions. In Fig. 6a, the fluorescence intensity of the *Lm* sensor at different concentrations of Hg^{2+} (ranging from 0 to 0.1 nM) is reported. The original fluorescence intensity of the *Lm* sensor was gradually quenched by the addition of mercury ions. A good linear trend is observed in the entire range of 0–0.1 nM. The linear regression equation was deduced as $y = 222624x + 1024$, with an R2 value of 0.9920, and the limit of detection (LOD) was calculated as 0.006 nM (Fig. 6b).

It is worth mentioning that, when comparing the limit of detection (LOD) of the *Lm* solid sensor with that of the *Lm* aqueous extract, the *Lm* solid sensor exhibited a lower LOD. In comparison with previously reported solid-state sensors for mercury ions, our sensor demonstrated a lower LOD (refer to Table S1). This outcome could be attributed to the presence of bioactive fluorescent components in *Lm* herbal tea (Nogués et al., 2000; Radu et al., 2019), which also significantly benefit from being entrapped within the Nafion structure of the solid sensor. The solid device offers several advantages: (i) easy operation, (ii) higher stability of the fluorescent dye when entrapped in the solid support, and (iii) portability, contributing to its extensive practical applications.

A schematic representation of the observed behavior is illustrated in Fig. 6c. When stimulated at 390 nm, the *Lm* sensors showed a high emission peak at 450 nm. Upon addition of mercury ions, the intensity of

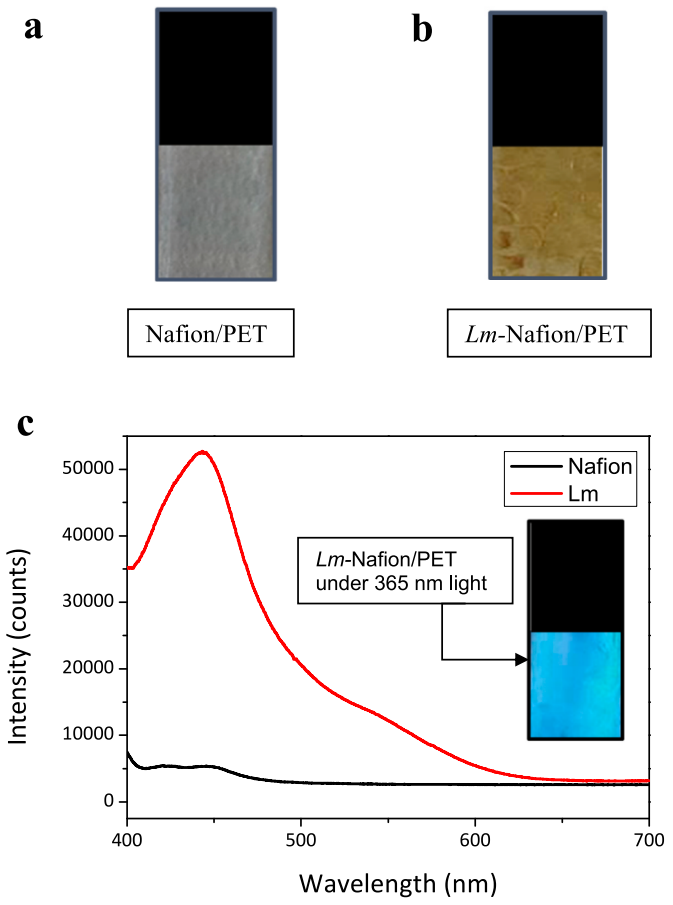

Fig. 5. Picture of the *Lavandula multifida* solid state sensor; **a)** Nafion/PET substrate; **b)** *Lm*-Nafion/PET under visible light; **c)** Fluorescence emission under excitation wavelength of 390 nm of *Lm*-Nafion/PET solid state sensor, compared to Nafion/PET. Inset shows a picture of the *Lm*-Nafion/PETsolid state device under UV lamp irradiation at 365 nm.

the fluorescence peak decreased and transitioned to the "off" state. This is likely due to the electrostatic interaction that leads to non-radiative recombination of excitations through electron transfer between the hydroxyl groups of *Lm* polyphenol receptors and Hg^{2+}, resulting in fluorescence quenching (Shuai et al., 2021; Pourreza et al., 2019).

However, it cannot be excluded that other binding modes may occur due to the interaction of mercury ions with organic functional groups containing oxygen, sulfur, and nitrogen atoms. These functional groups, which are largely present in the multitude of *Lm* phytochemicals, provide a high affinity towards Hg^{2+} ions. Therefore, a deeper study needs to be undertaken to confirm the above-illustrated mechanism for sensing mercury ions or to propose alternative mechanisms.

Additionally, the result reported above also suggests that the coexistence of most metal ions does not interfere with the complexation of Hg^{2+} with the hydroxyl groups of *Lm* polyphenol receptors and the subsequent fluorescence change.

3.6. Real sample analysis

The detection of mercury ions in environmental samples is a major concern due to their high toxicity and the serious health hazards they pose. In recent years, various strategies have been developed for the sensitive and selective detection of mercury in complex matrices such as seawater (Deshpande et al., 2022). As the measured pH of seawater (8.05) differs from that of distilled water, we prepared Hg^{2+} ion stock solutions in buffered solutions of this pH. To validate the feasibility and applicability of the fluorescent *Lm*-Nafion-PET sensor in determining

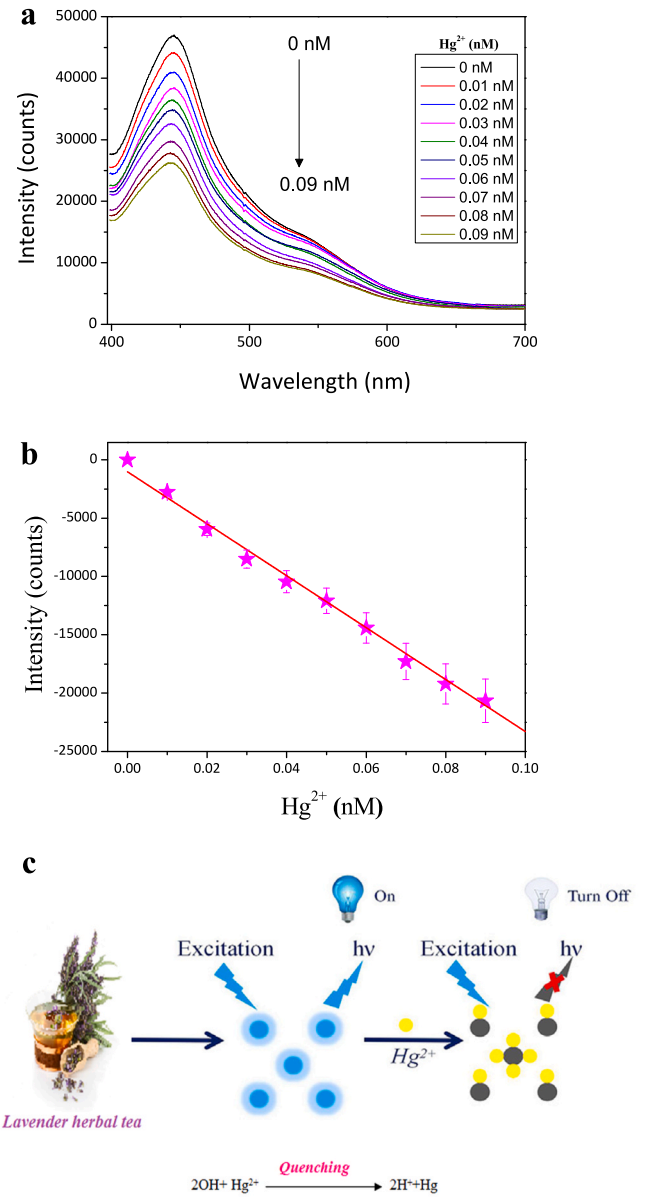

Fig. 6. Behavior of the *Lavandula multifida* solid-state sensor; **a)** response of the sensor to mercury ions; **b)** calibration curve with error bars derived from measurement carried in triplicate; **c)** mercury ions sensing mechanism with the *Lavandula multifida* sensor.

Hg^{2+} in real samples, we first verified the behavior of the Lm dye in seawater, confirming that its fluorescent characteristics are not altered in this medium.

Subsequently, the sensor was used to test a seawater sample taken from Acqualadroni, Messina, Italy. The concentration of mercury ions in this real sample was initially determined by atomic absorption spectroscopy and was found to be below the detection limit of this technique. Subsequently, mercury ions ranging from 0 to 3 fM were added to the seawater sample in a stepwise manner.

The initial fluorescence intensity was observed to decrease with the increase in Hg^{2+} concentration (Fig. 7a). A well-defined linear relationship was observed within the range of 0–3 fM, with a linear regression equation of $y = 47.964 + 5766.21x$, an R^2 value of 0.99562, and a limit of detection (LOD) of 0.25 fM (Fig. 7b). Based on measurements collected in triplicate, a RSD of 0.596% for mercury ion analysis in seawater was obtained, suggesting the potential use of the *Lm*-Nafion/

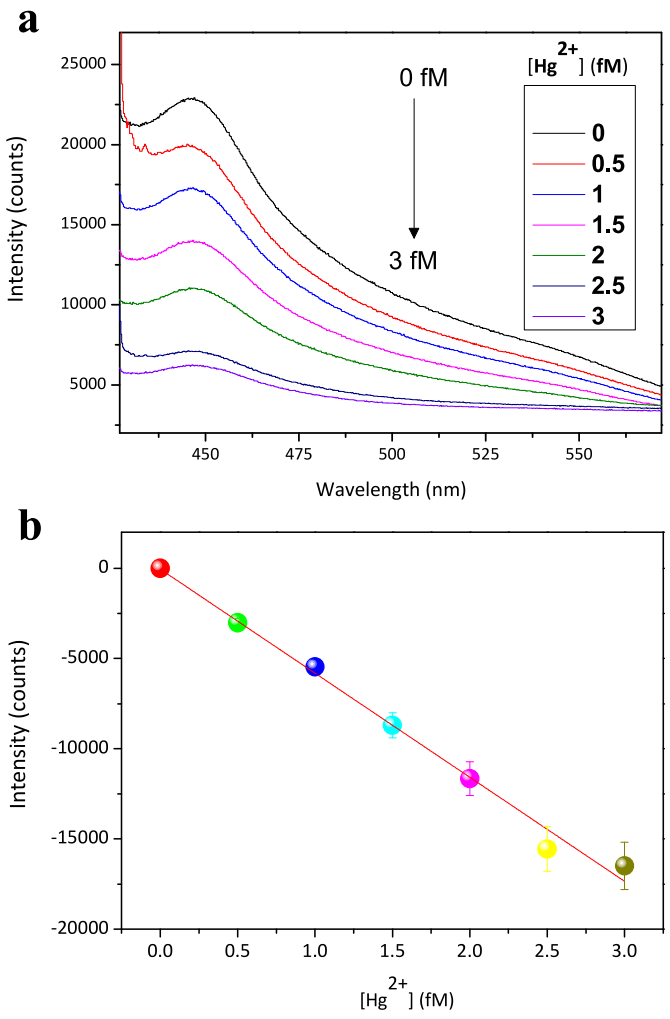

Fig. 7. a) *Lavandula multifida* sensor response to mercury in seawater; **b)** calibration curve with error bars derived from measurements carried in triplicate.

PET sensor for accurate Hg^{2+} detection in complex environmental samples.

4. Conclusion

In the present work, a natural, eco-friendly dye based on the herbal infusion of *Lavandula multifida* has been proposed for the first time. The prepared aqueous extract of *Lm* displayed high fluorescence and has been applied for the selective detection of Hg^{2+} ions in water with good sensitivity. By using *Lm* embedded in a Nafion matrix deposited on a flexible PET sheet as the substrate, a solid-state fluorescent sensor was successfully fabricated. The *Lm*-Nafion/PET sensor displays enhanced stability and extraordinary sensitivity to Hg^{2+} ions when tested in a real seawater sample. As the preparation of the sensor is simple and environmentally friendly, this work may open a new avenue for the development of fluorescent sensors based on plants at a low cost and characterized by high performance.

Declarations

Consent for publication

Not applicable.

Availability of data and materials

All data generated or analyzed during this study are included in this published article.

CRediT authorship contribution statement

MeryamChelly: Writing – original draft, Investigation, Conceptualization. **Sabrine Chelly:** Writing – original draft, Investigation, Conceptualization. **Angelo Ferlazzo:** Investigation. **Giovanni Neri:** Writing – review & editing, Supervision. **Hanen Bouaziz-Ketata:** Supervision.

Declaration of competing interest

The authors declare that they have no known competing financial interests or personal relationships that could have appeared to influence the work reported in this paper.

Data availability

Data will be made available on request.

Acknowledgements

Sincere appreciation and heartfelt thanks are warmly expressed to Faiçal CHELLY,who helped with the plant collection. This work has been partially funded by European Union (NextGeneration EU), through the MUR-PNRR project SAMOTHRACE (ECS00000022).

Appendix A. Supplementary data

Supplementary data to this article can be found online at https://doi.org/10.1016/j.chemosphere.2024.141409.

References

Adair, L.D., et al., 2022. An introduction to small molecule fluorescent sensors. Mol. Fluoresc. Sens. Cell. Stud 1, 35. https://doi.org/10.1002/9781119749844.ch1.
Cao, H., et al., 2021. Available technologies on improving the stability of polyphenols in food processing. F. Front. 2, 109–139. https://doi.org/10.1002/fft2.65.
Chatenoux, B., et al., 2015. Integration of Climate Change Variability into National GIZC Strategies: "Contribution to the Updating of the Integrated Management Plan for Coastal Zones of the Kerkennah Archipelago", GRID-Geneva. Plan Bleu/RAC and GWP Med.
Chelly, M., et al., 2021. Synthesis of silver and gold nanoparticles from *Rumex roseus* plant extract and their application in electrochemical sensors. Nanomaterials 11, 739. https://doi.org/10.3390/nano11030739.
Cinnirella, S., et al., 2019. Mercury concentrations in biota in the Mediterranean Sea, a compilation of 40 years of surveys. Sci. Data 6, 205. https://doi.org/10.1038/s41597-019-0219-y.
Członka, S., et al., 2021. Polyurethane hybrid composites reinforced with lavender residue functionalized with kaolinite and hydroxyapatite. Materials 415. https://doi.org/10.3390/ma14020415.
Demchenko, A.P., 2008. Introduction to Fluorescence Sensing. Springer Sci. Bus. Med.
Deshpande, K., et al., 2022. Selective determination of mercury (II) in coastal water using bio-functionalized gold nanoparticles. Journal of Water and Environmental Nanotechnology 7, 370–379. https://doi.org/10.22090/jwent.2022.561201.1555.
Dhivya, S.M., et al., 2017. UV-Vis spectroscopic and FTIR analysis of *Sarcostemmabrevistigma*, wight and arn. Int. J. Herb. Med. 9, 46–49. https://doi.org/10.22159/ijcpr.2017v9i3.18890.
Dobros, N., et al., 2022. Phytochemical profile and antioxidant activity of *Lavandula angustifolia* and *Lavandula x intermedia* cultivars extracted with different methods. Antioxidants 711. https://doi.org/10.3390/antiox11040711.
Donaldson, L., 2020. Autofluorescence in plants. Molecules 25, 2393. https://doi.org/10.3390/molecules25102393.
Du, F., et al., 2019. A highly sensitive and selective "on-off-on" fluorescent sensor based on nitrogen doped graphene quantum dots for the detection of Hg^{2+} and paraquat. Sens. Actuators, B 288, 96–103. https://doi.org/10.1016/j.snb.2019.02.109.
He, X.L., et al., 2015. Composition and color stability of anthocyanin-based extract from purple sweet potato. Food Sci. Technol. 35, 468–473. https://doi.org/10.1590/1678-457X.6687.
https://www.sigmaaldrich.com/TN/en/technical-documents/technical-article/analytical-chemistry/photometry-and-reflectometry/ir-spectrum-table.

Huang, C., et al., 2019. Synthesis of carbon quantum dot nanoparticles derived from byproducts in bio-refinery process for cell imaging and *in vivo* bioimaging. Nanomaterials 9, 387. https://doi.org/10.3390/nano9030387.

Iannazzo, D., et al., 2021. Electrochemical and fluorescent properties of crown ether functionalized graphene quantum dots for potassium and sodium ions detection. Nanomaterials 11, 2897. https://doi.org/10.3390/nano11112897.

Javaid, M., et al., 2021. Sensors for dailylife: a review. Sens. Int. 2, 100121. https://doi.org/10.1016/j.sintl.2021.100121.

Jiang, Y., et al., 2021. Novel fluorescent probe based on dicoumarin for rapid on-site detection of Hg^{2+} in loess. Spectrochim. Acta, Part A 251, 119438. https://doi.org/10.1016/j.saa.2021.119438.

Kageyama, A., et al., 2012. Antidepressant-like effects of an aqueous extract of lavender (*Lavandula angustifolia* Mill.) in rats. Food Sci. Technol. Res. 18, 473–479. https://doi.org/10.3136/fstr.18.473.

Kim, S.H., et al., 2013. Characterization of crystalline cellulose in biomass: basic principles, applications, and limitations of XRD, NMR, IR, Raman, and SFG. Kor. J. Chem. Eng. 30, 2127–2141. https://doi.org/10.1007/s11814-013-0162-0.

Lang, M., et al., 1991. Fluorescence emission spectra of plant leaves and plant constituents. Radiat. Environ. Biophys. 30, 333–347. https://doi.org/10.1007/BF01210517.

Locquet, N., et al., 2006. 3D fluorescence spectroscopy and its applications. Encycl. Anal. Chem. 1–39. https://doi.org/10.1002/9780470027318.a9540.

Lopes, C.L., et al., 2018. Phenolic composition and bioactivity of *Lavandula pedunculata* (Mill.) Cav. samples from different geographical origin. Molecules 23, 1037. https://doi.org/10.3390/molecules23051037.

Marchini, E., et al., 2022. Electrodeposited PEDOT/Nafion as catalytic counter electrodes for cobalt and copper bipyridyl redox mediators in dye-Sensitized solar cells. ACS Omega7 29181–29194. https://doi.org/10.1021/acsomega.2c03229.

Mohan, H., et al., 1989. Optical absorption and emission studies on laser dye incorporated in Nafion membrane. Photochem. Photobiol. 49, 395–399. https://doi.org/10.1111/j.1751-1097.1989.tb09185.x.

Neji, M., et al., 2018. Floristic diversity and vegetation patterns along disturbance gradient in arid coasts in southern Mediterranean: case of the Gulf of Gabès, southern Tunisia. Arid Land Res. Manag. 32, 291–315. https://doi.org/10.1080/15324982.2018.1431332.

Nogués, S., et al., 2000. Effects of drought on photosynthesis in Mediterranean plants grown under enhanced UV-B radiation. J. Exp. Bot. 51, 1309–1317. https://doi.org/10.1093/jxb/51.348.1309.

Pourreza, N., et al., 2019. Green synthesized carbon quantum dots from Prosopis juliflora leaves as a dual off-on fluorescence probe for sensing mercury (II) and chemet drug. Mater. Sci. Eng. C. 98, 887–896. https://doi.org/10.1016/j.msec.2018.12.141.

Radu, D., et al., 2019. Investigations on thermal degradation of phytochemicals from lavender extract, Ann. Univ. Dunarea Jos Galati, Fascicle VI. Food Technol. 43, 33–47. https://doi.org/10.35219/foodtechnology.2019.2.03.

Rebollar, E., et al., 2014. Physicochemical modifications accompanying UV laser induced surface structures on poly (ethylene terephthalate) and their effect on adhesion of mesenchymal cells. Phys. Chem. Chem. Phys. 16, 17551–17559. https://doi.org/10.1039/C4CP02434F.

Satira, A., et al., 2021. Hydrothermal carbonization as sustainable process for the complete upgrading of orange peel waste into value-added chemicals and bio-carbon materials. Appl. Sci. 11, 10983. https://doi.org/10.3390/app112210983.

Şenol, A.M., et al., 2023. A simple fluorescent "Turn off-on" sensor based on P, N-doped graphene quantum dots for Hg^{2+} and Cysteine determination. Sensor Actuator Phys. 356, 114362. https://doi.org/10.1016/j.sna.2023.114362.

Shuai, H., et al., 2021. Fluorescent sensors for detection of mercury: from small molecules to nanoprobes. Dyes Pigments 187, 109125. https://doi.org/10.1016/j.dyepig.2020.109125.

Singh, V., et al., 2015. White light emission from vegetable extracts. Sci. Rep. 5, 1–9. https://doi.org/10.1038/srep11118.

Sridhar, A., et al., 2021. Techniques and modeling of polyphenol extraction from food: a review. Environ. Chem. Lett. 19, 3409–3443. https://doi.org/10.1007/s10311-021-01217-8.

Sun, X., et al., 2021. Conversional fluorescent kiwi peel phenolic extracts: sensing of Hg^{2+} and Cu^{2+}, imaging of HeLa cells and their antioxidant activity. Spectrochim. Acta Part A Mol. Biomol. Spectrosc. 244, 118857. https://doi.org/10.1016/j.saa.2020.118857.

Vasileva, I., et al., 2018. Effect of lavender (*Lavandula angustifolia*) and melissa (*Melissa Officinalis*) waste on quality and shelf life of bread. Food Chem. 253, 13–21. https://doi.org/10.1016/j.foodchem.2018.01.131.

Wang, Y., et al., 2021. Fluorescent probe for mercury ion imaging analysis: strategies and applications. Chem. Eng. J. 406, 127166. https://doi.org/10.1016/j.cej.2020.127166.

Wei, J., et al., 2018. Sol–gel synthesis of metal–phenolic coordination spheres and their derived carbon composites. Angew. Chem. 130, 9986–9991. https://doi.org/10.1002/ange.201805781.

Yang, S., et al., 2022. Water-dispersible chlorophyll-based fluorescent material derived from willow seeds for sensitive analysis of copper ions and biothiols in food and living cells. J. Photochem. Photobiol. Chem. 425, 113664. https://doi.org/10.1016/j.jphotochem.2021.113664.

Yılmaz, D.D., et al., 2021. Colorimetric detection of mercury ion using chlorophyll functionalized green silver nanoparticles in aqueous medium. Surf. Interface. 22, 100840. https://doi.org/10.1016/j.surfin.2020.100840.

Zhu, F., 2015. Interactions between starch and phenolic compound. Trends Food Sci. Technol. 43, 129–143. https://doi.org/10.1016/j.tifs.2015.02.003.